Annals of Nuclear Medicine Vol. 20, No. 6, 417–424, 2006

Synthesis and evaluation of vesamicol analog (–)-*o*-[^{11}C]methylvesamicol as a PET ligand for vesicular acetylcholine transporter

Kazunori KAWAMURA,*,** Kazuhiro SHIBA,*** Hideo TSUKADA,****
Shingo NISHIYAMA,**** Hirofumi MORI*** and Kiichi ISHIWATA*

*Positron Medical Center, Tokyo Metropolitan Institute of Gerontology
**SHI Accelerator Service Ltd.
***Advanced Science Research Center, Kanazawa University
****Central Research Laboratory, Hamamatsu Photonics K.K.

(–)-*o*-Methylvesamicol ((–)-OMV) exhibited *in vitro* a high affinity for vesicular acetylcholine transporter (VAChT) (*K*i, 6.7 nM) and a relatively low affinity for sigma$_1$ receptor (*K*i, 33.7 nM). We prepared (–)-[^{11}C]OMV by a palladium-promoted cross-coupling reaction using [^{11}C]methyl iodide, in a radiochemical yield of 38 ± 6.9% (n = 3), a radiochemical purity of 98 ± 2.3% (n = 5), and a specific activity of 11 ± 7.0 TBq/mmol at 30 minutes after EOB (n = 5). Then, we evaluated *in vivo* whether (–)-[^{11}C]OMV has properties as a PET radioligand for mapping VAChT. In rats, the brain uptake of (–)-[^{11}C]OMV was 1.1%ID/g at 5 minutes postinjection, and was retained of a high level for 60 minutes. The brain uptake was significantly inhibited by the co-injection (500 nmol/kg) of cold (–)-OMV (58–66%), (–)-vesamicol (57–65%), and two sigma receptor ligands with modulate affinities for VAChTs: SA4503 (56–71%) and haloperidol (39–64%) in all of the brain regions, including the cerebellum with a low density of VAChTs, but not of sigma$_1$-selective ligand (+)-pentazocine. However, the pretreatment with a large excess amount of (±)-pentazocine (50 μmol/kg) reduced the uptake in a different manner in the brain regions: 25% reduction in the striatum with a high density of VAChTs, and a 50–55% reduction in the other regions with a lower density of VAChTs. *Ex vivo* autoradiography using (–)-[^{11}C]OMV showed a similar regional brain distribution of [^{3}H](–)-vesamicol. In the PET study of the monkey brain, the regional brain distribution pattern of (–)-[^{11}C]OMV was different from that of [^{11}C]SA4503. The uptake of (–)-[^{11}C]OMV was relatively higher in the striatum, was reversible, and an apparent equilibrium state was found at 20–40 minutes. In conclusion, (–)-[^{11}C]OMV exhibited appropriate brain kinetics during the time frame of ^{11}C-labeled tracers and bound mainly to VAChTs; however, the binding to sigma$_1$ receptors was not disregarded. Therefore, (–)-[^{11}C]OMV-PET together with help of [^{11}C]SA4503-PET may evaluate VAChTs.

Key words: (–)-*o*-[^{11}C]methylvesamicol, VAChT, PET, vesamicol

INTRODUCTION

THE VESICULAR ACETYLCHOLINE TRANSPORTER (VAChT) is localized exclusively in cholinergic neurons[1–4] and thus has been established as a reliable marker for presynaptic cholinergic terminals. Consequently, a selective radioligand for VAChT may be used as a tool for studying the function of cholinergic neurons with positron emission tomography (PET) and single photon emission computed tomography (SPECT).

2-(4-Phenylpiperidino)cyclohexanol (vesamicol) has been reported to bind to VAChTs on presynaptic acetylcholine storage vesicles.[5,6] Therefore, many radioligands based on vesamicol have been developed for mapping VAChTs with PET[7–13] and SPECT.[14–18] Substituted

Received November 30, 2005, revision accepted May 16, 2006.

For reprint contact: Kiichi Ishiwata, Ph.D., Positron Medical Center, Tokyo Metropolitan Institute of Gerontology, Naka-cho 1–1, Itabashi-ku, Tokyo 173–0022, JAPAN.
E-mail: ishiwata@pet.tmig.or.jp

positions and optical isomerization of the vesamicol derivatives altered their affinities for VAChTs and sigma receptors.[11,19] Shiba et al. synthesized (–)-*o*-methylvesamicol ((–)-OMV), wihch exhibited a high affinity for VAChTs (*K*i, 6.7 nM) and a relatively low affinity for sigma$_1$ receptor *in vitro* (*K*i for sigma$_1$, 33.7 nM; *K*i for sigma$_2$, 266 nM) (Table 1).[20] The VAChT/sigma$_1$ receptor selectivity of (–)-OMV (5.0) would not be sufficient for VAChTs; however, in general, a *K*i = 33.7 nM is not optimal if one is seeking PET and SPECT radioligands.

Recently, Efange et al. reported [^{18}F](+)-4-fluorobenzyltrozamicol ([^{18}F](+)-FBT) as a potential PET ligand for mapping VAChTs.[10] (+)-FBT was found to have a high affinity (*K*i, 0.22 nM) for VAChTs and a lower affinity for sigma$_1$ receptors (*K*i, 21.6 nM) and sigma$_2$ receptors (*K*i, 35.9 nM).[21] In the *in vivo* study, [^{18}F](+)-FBT showed a high uptake and a slow rate of washout from the striatum of rats[10] and monkeys.[21] Compared with (+)-FBT, (–)-OMV has a lower affinity for VAChTs, a slightly lower affinity for sigma$_1$ receptors and much lower affinity for sigma$_2$ receptors. Therefore, it is considered that (–)-*o*-[^{11}C]methylvesamicol ((–)-[^{11}C]OMV) shows a faster rate of washout from the striatum than [^{18}F](+)-FBT without affinity for sigma receptors. The brain kinetics that the receptor-ligand binding reaches the apparent equilibrium state during the time-scale for PET measurement is preferable for quantitative analysis. Negligible binding of (–)-[^{11}C]OMV to sigma receptors is also expected. Here, we prepared (–)-[^{11}C]OMV by substitution of the trimethylstannyl group with [^{11}C]methyl iodide in a palladium-promoted cross-coupling reaction (Fig. 1)[22] and evaluated *in vivo* in rats whether (–)-[^{11}C]OMV has properties as a PET radioligand for mapping VAChT, or whether it shows affinity for both VAChTs and sigma receptors. We also performed PET imaging of the monkey brain with (–)-[^{11}C]OMV, compared with the PET imaging with [^{11}C]SA4503 that has been developed as a selective PET ligand for mapping sigma$_1$ receptors.[23–25]

Table 1 *In vitro* affinities of (–)-OMV, (–)-vesamicol and three sigma receptor ligands for vesicular acetylcholine transporter (VAChT) and sigma receptors

	*K*i* (nM)		
	VAChT[#]	Sigma$_1$ receptor[†]	Sigma$_2$ receptor[$]
(–)-OMV	6.7 ± 1.6	33.7 ± 5.9	266 ± 28
(+)-OMV	22.5 ± 2.0	10.7 ± 2.0	218 ± 20
(–)-Vesamicol	4.4 ± 0.6	73.8 ± 11.2	346 ± 37
SA4503	50.2 ± 7.2	4.4 ± 1.0	242 ± 17
Haloperidol	41.4 ± 17.6	2.6 ± 0.8	167 ± 19
(+)-Pentazocine	315 ± 121	5.5 ± 2.0	2470 ± 150

Data from Shiba et al.[20]

*Values are the average of three experiments.

[#]Rat cerebral membranes were incubated with [^{3}H](–)-vesamicol in 50 mmol/*l* Tris-HCl (pH 7.8) for 60 minutes at 37°C in the presence of 200 nmol/*l* DTG to mask the sigma receptors. [†]Rat cerebral membranes were incubated with [^{3}H](+)-pentazocine in 50 mmol/*l* Tris-HCl (pH 7.8) for 90 minutes at 37°C. [$]Rat liver membranes were incubated with [^{3}H]DTG in 50 mmol/*l* Tris-HCl (pH 7.8) for 90 minutes at 37°C in the presence of 0.001 mmol/*l* (+)-pentazocine to mask the sigma$_1$ receptors.

MATERIALS AND METHODS

General

(–)-Vesamicol and haloperidol were purchased from Sigma Chemical (St. Louis, MO). SA4503 and (+)-pentazocine were provided from M's Science (Kobe, Japan). (±)-Pentazocine (PENTAGIN® injection) was purchased from Sankyo (Tokyo, Japan). (–)-OMV and (–)-2-(4-(2-trimethylstannylphenyl)piperidino)cyclohexanol ((–)-*o*-trimethylstannyl-vesamicol) were synthesized as described previously.[20] All chemicals were obtained from commercial sources.

Male Wistar rats were obtained from Tokyo Laboratory Animals (Tokyo, Japan). Animal experiments were carried out in compliance with the Guidelines for Animal Care and Use Committee of the Tokyo Metropolitan Institute of Gerontology.

Two male rhesus monkeys (*Macaca mulatta*, 7 years old, 6.4 and 6.6 kg) were used for the PET measurements. They were trained to sit on a chair twice a week for more than three months. The study was performed in accordance with recommendations of the US National Institute of Health and the guidelines of the Central Research Laboratory, Hamamatsu Photonics K.K.

Radiolabeling of (–)-[^{11}C]OMV

A solution of tris(dibenzylideneacetone)dipalladium(0) (2.8–3.4 mg, 3.0–3.6 μmol), tri(*o*-tolyl)phosphine (3.7–4.0 mg, 12–13 μmol) in *N*,*N*-dimethylformamide (DMF) (0.2 m*l*) was prepared in a dry septum equipped vial and heated for a few minutes (until the color in the solution changed to yellow), and then added to the mixture of copper chloride (1.2–3.0 mg, 12–30 μmol), potassium carbonate (1.7–2.5 mg, 12–18 μmol) and (–)-*o*-trimethylstannyl-vesamicol (0.6 mg) in DMF (0.2 m*l*). [^{11}C]Methyl iodide was produced from [^{11}C]CO_2 with an automated system (Sumitomo Heavy Industries, Tokyo, Japan) and was trapped in the mixture of DMF (0.4 m*l*) with air cooling. The reaction mixture was heated at 80°C for 3 minutes. After adding 1.2 m*l* of high-performance liquid chromatography (HPLC) eluent [acetonitrile/ 50 mmol/*l* ammonium acetate, (30/70, v/v)], the reaction mixture was passed through the glass filter (20 μm) and followed by injection onto the preparative HPLC: YMC-Pack ODS-A column (10 mm inner diameter (i.d.) × 250 mm length, YMC, Kyoto, Japan) with a mobile phase of acetonitrile/ 50 mmol/*l* ammonium acetate (30/70) at a flow rate of 5.0 m*l*/minute (UV detector at 260 nm). The

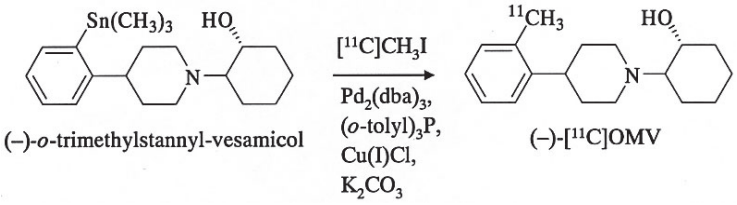

Fig. 1 Synthesis of (–)-[^{11}C]OMV.

retention time of (–)-[^{11}C]OMV was 17 minutes. The fraction of (–)-[^{11}C]OMV was collected and evaporated to dryness. The residue was dissolved in physiological saline. The final product was analyzed by HPLC using a TSKgel super-ODS column (4.6 mm i.d. × 100 mm length, Toso, Tokyo, Japan) with a mobile phase of acetonitrile/ 50 mmol/*l* acetic acid/ 50 mmol/*l* ammonium acetate (25/37.5/37.5, v/v/v) at a flow rate of 1.0 m*l*/ minute (UV detector at 260 nm). The retention time of (–)-[^{11}C]OMV was 4.4 minutes.

Tissue distribution in rats

(–)-[^{11}C]OMV (9.7 MBq/2.2 nmol) was intravenously injected into Wistar rats (7 weeks old, 210–250 g). Rats were sacrificed by cervical dislocation 5, 15, 30 and 60 minutes after injection (n = 4). The blood was collected by heart puncture, and tissues were harvested and weighed. The ^{11}C radioactivity in the samples was measured with an auto-gamma scintillation counter. The tissue uptake of ^{11}C was expressed as the percentage of the injected dose per gram of tissue (%ID/g).

To determine the specific binding, we performed the blocking experiment by co-injection with cold (–)-OMV, (–)-vesamicol, SA4503 (sigma$_1$ receptor ligand), haloperidol (non-selective sigma receptor ligand) and (+)-pentazocine (sigma$_1$ receptor ligand), and by pretreatment with (±)-pentazocine (PENTAGIN® injection) (non-selective sigma receptor ligand). A mixture of (–)-[^{11}C]OMV (9.9 MBq/0.68 nmol) and one of blockers, except for (±)-pentazocine, at a dose of 500 nmol/kg in 0.2 m*l* physiological saline/dimethyl sulfoxide (1/1, v/v) was injected into the rats. In the other group of rats, 50 μmol/ kg of (±)-pentazocine was intravenously administrated 10 minutes prior to the tracer injection (14 MBq/ 0.87 nmol). The rats were sacrificed by cervical dislocation 30 minutes after injection (n = 4–6, 7–8 weeks old, 230–270 g). The sample collection and measurement were performed as described above.

Metabolite study in rats

(–)-[^{11}C]OMV (111–118 MBq/7.2–25 nmol) was intravenously injected into rats (7–8 weeks old, 240–270 g), and 15 (n = 3) or 30 (n = 1) minutes later they were sacrificed by cervical dislocation. Blood was removed by heart puncture using a heparinized syringe, and the brain was removed. The blood was centrifuged at 7,000 × *g* for 1 minute at 4°C to obtain the plasma, which was denatured with a 1/3 equivalent volume of 20% trichloroacetic acid (TCA) in acetonitrile. The mixture was centrifuged in the same condition, and the precipitate was re-suspended in 0.5 m*l* of 10% TCA in acetonitrile followed by centrifugation. This procedure was repeated three times. The brain was homogenized in 1 m*l* of 20% TCA in acetonitrile/water (1/1, v/v). The homogenate was treated as described above. The combined supernatant was analyzed by HPLC with a radioactivity detector (Radiomatic 150TR, Packard, Meriden, CT). A Radial-Pak C18 column equipped in an RCM 8 × 10 module (8 mm × 100 mm, Waters, Milford, MA) was used with a mixture of 35% acetonitrile and 65% 50 mmol/*l* acetic acid/sodium acetate (1/1) at a flow rate of 2 m*l*/minute.

Ex vivo *autoradiography in rats*

Ex vivo autoradiography of the brain was carried out in rats. (–)-[^{11}C]OMV (111 MBq/7.2 nmol) was intravenously injected into the rat (8 weeks old, 270 g). The rat was sacrificed by cervical dislocation at 30 minutes after injection. The brain was rapidly dissected, frozen, and coronally cut into 20 μm thick sections using a cryotome (Bright Instrument, Huntingdon, UK). The brain sections were dried on a hot plate at 60°C and were apposed to a storage phosphor screen (PhosphorImager SI system, Molecular Dynamics, Sunnyvale, CA) for 2 hours.

PET measurement in the monkey brain

A monkey was fixed on a PET camera, a model SHR-7700 (Hamamatsu Photonics K.K., Hamamatsu, Japan), which acquires 31 slices at a center-to-center interval of 3.6 mm with a resolution of 2.6 mm full width at half maximum in the transaxial plane. (–)-[^{11}C]OMV (745 MBq/ 8.8 nmol) was injected into the monkey through a posterior tibial vein cannula. The PET scanning was performed for 61 minutes with 6 time frames at 10 second intervals, 6 time frames at 30 seconds, 12 time frames at 1 minute, followed by 15 time frames at 3 minutes. In the other monkey, the PET study with [^{11}C]SA4503 (537 MBq/8.4 nmol) was performed in the same way. Regions of interest were placed on the striatum, occipital cortex, frontal cortex, temporal cortex and cerebellum. The decay-corrected radioactivity was expressed as the percentage of the injected dose per m*l* tissue volume (%ID/m*l*).

Table 2 Tissue distribution of radioactivity after intravenous injection of (–)-[^{11}C]OMV in rats

	Radioactivity level (%ID/g)*			
	5 minutes	15 minutes	30 minutes	60 minutes
Blood	0.09 ± 0.01	0.06 ± 0.01	0.05 ± 0.004	0.04 ± 0.003
Heart	0.70 ± 0.06	0.38 ± 0.04	0.32 ± 0.02	0.20 ± 0.01
Lung	3.43 ± 0.53	2.15 ± 0.51	1.81 ± 0.07	1.00 ± 0.16
Liver	0.53 ± 0.05	0.61 ± 0.08	0.67 ± 0.16	0.68 ± 0.07
Pancreas	1.75 ± 0.40	2.51 ± 0.46	2.39 ± 0.55	2.21 ± 0.25
Spleen	1.03 ± 1.06	1.22 ± 0.11	1.15 ± 0.11	0.88 ± 0.07
Kidney	2.30 ± 0.89	1.56 ± 0.08	1.25 ± 0.02	0.86 ± 0.10
Small intestine	1.28 ± 0.12	1.82 ± 0.35	1.76 ± 0.38	1.85 ± 0.10
Muscle	0.32 ± 0.06	0.29 ± 0.09	0.25 ± 0.05	0.21 ± 0.03
Brain	1.13 ± 0.09	0.94 ± 0.11	0.98 ± 0.09	0.80 ± 0.06

*Radioactivity levels are represented as the mean % injection dose per gram of tissue ± S.D. (n = 4).

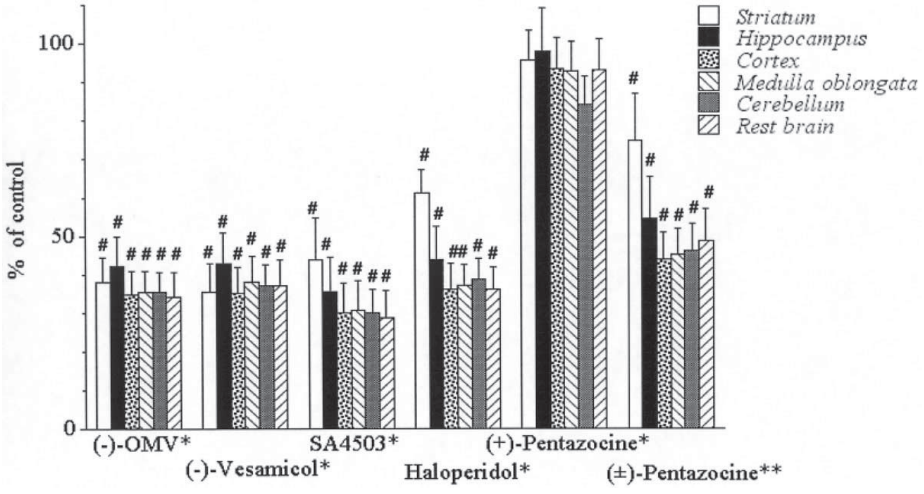

Fig. 2 The blocking effects of (–)-OMV, (–)-vesamicol, SA4503, haloperidol, (+)-pentazocine and (±)-pentazocine on the regional brain distribution of (–)-[^{11}C]OMV in rats at 30 minutes after intravenous injection. *Co-injected dose with (–)-OMV, (–)-vesamicol and (+)-pentazocine was 500 nmol/kg. **Pretreatment dose with (±)-pentazocine was 50 μmol/kg. Radioactivity levels are represented as the mean % injection dose per gram of tissue (%ID/g) ± S.D. (n = 4–6). $^{\#}p < 0.005$, Student's t-test compared with the control.

RESULTS

Radiolabeling of (–)-[^{11}C]OMV

(–)-[^{11}C]OMV was synthesized by methylation of the (–)-*o*-trimethylstannyl-vesamicol with [^{11}C]methyl iodide in a palladium-promoted cross-coupling reaction (Fig. 1).[22] The total synthesis time was about 30 minutes. The decay corrected radiochemical yield was 38 ± 6.9% (n = 3) calculated from [^{11}C]methyl iodide, and the radiochemical purity determined by analytical HPLC was 98 ± 2.3% (n = 5). The specific activity was 11 ± 7.0 TBq/mmol (n = 5) at 30 minutes after the end of bombardment.

Tissue distribution in rats

The tissue distribution of the radioactivity after injection of (–)-[^{11}C]OMV into rats is summarized in Table 2. The initial uptake of (–)-[^{11}C]OMV was high in the lung (3.4%ID/g) and kidney (2.3%ID/g), while the uptake at 60 minutes was high in the pancreas (2.2%ID/g) and small intestine (1.8%ID/g). The uptake in the brain showed a tendency to decrease over 60 minutes, and the radioactivity levels of (–)-[^{11}C]OMV decreased in the blood, heart, lung, kidney and muscle over 60 minutes. The uptake levels in the pancreas, spleen and small intestine increased until 15 minutes and then decreased for 60 minutes. In the liver, the uptake slightly increased for 60 minutes.

The regional distribution of (–)-[^{11}C]OMV in the brain and the blocking effects of (–)-OMV, (–)-vesamicol, and three sigma receptor ligands on the uptake were investigated at 30 minutes after the tracer injection. In the control group, the uptake values of the striatum, hippocampus, cerebral cortex, medulla oblongata, cerebellum and the rest of brain were 1.07 ± 0.14, 0.97 ± 0.12, 1.16 ± 0.12,

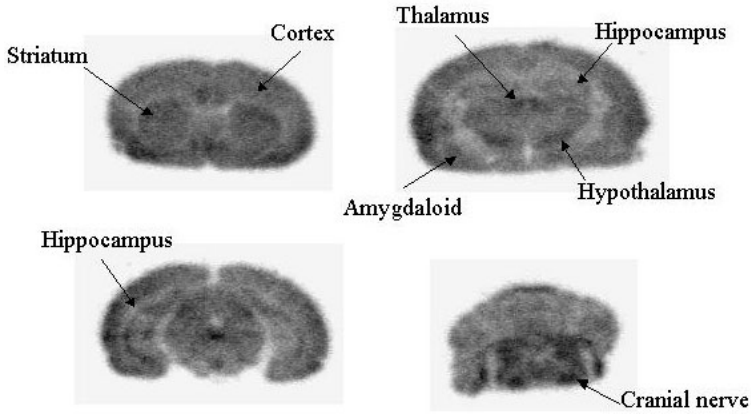

Fig. 3 *Ex vivo* autoradiography of the coronal sections of the rat brain at 15 minutes after injection of (–)-[^{11}C]OMV.

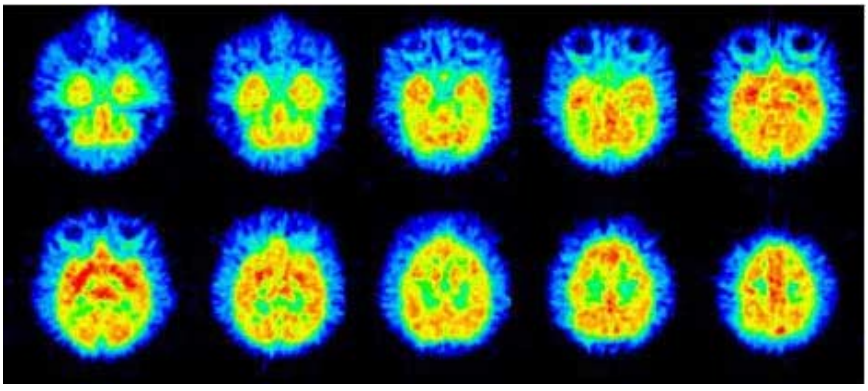

Fig. 4 The brain images of (–)-[^{11}C]OMV of a conscious monkey. The PET images of (–)-[^{11}C]OMV were acquired for 45 minutes starting at 60 minutes after injection.

1.21 ± 0.12, 0.97 ± 0.10 and 1.08 ± 0.12, respectively. As shown in Figure 2, the uptake of (–)-[^{11}C]OMV was significantly decreased by the co-injection of (–)-OMV (34–42% of control), (–)-vesamicol (35–43% of control), SA4503 (29–44% of control), and haloperidol (36–61% of control) at a dose of 500 nmol/kg in all of the brain regions. The blocking effects of (–)-OMV and (–)-vesamicol were equivalent in all of the regions (57–66% blockade of control), whereas those of each sigma receptor ligand were smaller in the striatum (56% by SA4503 and 39% by haloperidol) than in the other regions (65–71% by SA4503 and 66–74% by haloperidol). On the other hand, co-injection of (+)-pentazocine at the dose of 500 nmol/kg did not reduce the uptake of (–)-[^{11}C]OMV in any of the brain regions, although the uptake in the cerebellum seemed to be reduced. However, pretreatment with a large excess of (±)-pentazocine (50 μmol/kg) significantly decreased the uptake of (–)-[^{11}C]OMV in all of the brain regions, and the effect was relatively small in the striatum (25% reduction) as compared to that in the other regions (50–55%).

Metabolite study in rats

Metabolite analysis was carried out in the brain and plasma at 15 minutes and 30 minutes after injection. The recovery of the radioactivity in the HPLC analysis was essentially quantitative. At 15 minutes after injection of (–)-[^{11}C]OMV, the percentages of the unchanged form in the brain and in the plasma were 96 ± 1.3% and 58 ± 0.5% (n = 3), respectively, and at 30 minutes after injection, that in the brain and in the plasma were 98% and 58% (n = 1), respectively.

Ex vivo *autoradiography in rats*

Figure 3 shows the coronal images of the rat brain visualized by *ex vivo* autoradiography with (–)-[^{11}C]OMV at 15 minutes after tracer injection. A slightly higher ^{11}C density was observed in the striatum, pyramidal cell layer of the hippocampus, hypothalamus, thalamus and nuclei of the cranial motor nerves. A moderate ^{11}C density was observed in the cortex and amygdaloid.

PET measurement in the monkey brain

Figure 4 shows PET images of (–)-[^{11}C]OMV in the

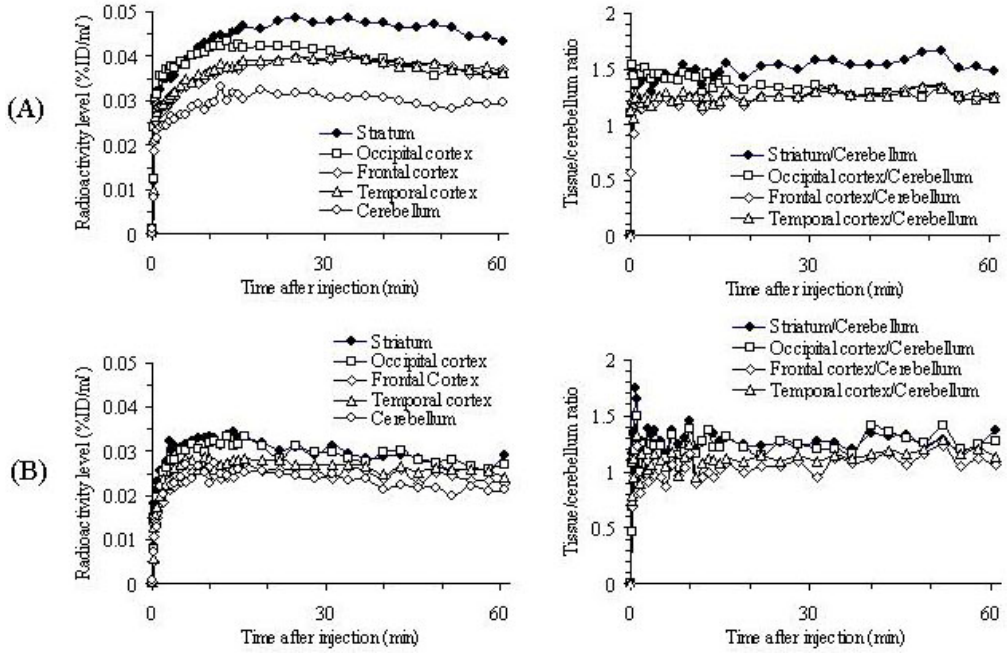

Fig. 5 Time-activity curves of the regional brain tissues and the uptake ratio of tissue-to-cerebellum after intravenous injection of (–)-[^{11}C]OMV (A) and [^{11}C]SA4503 (B) in a conscious monkey using PET. The radioactivity levels are expressed as the percent of injected dose per m*l* tissue volume.

monkey brain (images of (–)-[^{11}C]SA4503 not shown[24]). The uptake of (–)-[^{11}C]OMV was relatively higher in the striatum. In Figure 5, the time-activity curves of (–)-[^{11}C]OMV and [^{11}C]SA4503 showed different regional distribution patterns. (–)-[^{11}C]OMV showed the highest uptake in the striatum and lowest uptake in cerebellum, while the regional differences in the uptake of (–)-[^{11}C]SA4503 were small. The binding of the two tracers was reversible, and an apparent equilibrium state was found at 20–40 minutes for (–)-[^{11}C]OMV and at 5–15 minutes for [^{11}C]SA4503.

DISCUSSION

Synthesis of (–)-[^{11}C]OMV was achieved by a palladium-promoted cross-coupling reaction with [^{11}C]methyl iodide.[22] (–)-[^{11}C]OMV was prepared in a sufficient radiochemical yield (38 ± 6.9%) for the *in vivo* studies. The specific radioactivity was relatively low (11 ± 7.0 TBq/mmol at 30 minutes after the end of bombardment), compared with the other ^{11}C-labeled tracers prepared in our laboratory, such as [^{11}C]SA4503.[23] However, this specific radioactivity is sufficient for the *in vivo* studies. The reason for the low specific radioactivity might be explained by the fact that a cross-coupling between one of the methyl groups on the tin and the nucleoside part can occur yielding (–)-OMV.[26]

Vesamicol and its analogs have been reported to bind to VAChTs and sigma receptors.[27] The issue addressed in the present study is whether (–)-[^{11}C]OMV specifically binds to VAChTs (*K*i, 6.7 nM),[20] but not to sigma$_1$ receptors (*K*i for sigma$_1$, 33.7 nM; *K*i for sigma$_2$, 266 nM)[20] *in vivo*.

The density of VAChTs was the highest in the striatum and low in the cerebellum,[11,28,29] whereas sigma$_1$ receptors are distributed more uniformly in the brain.[30] In a blocking study, (–)-OMV, (–)-vesamicol and two sigma$_1$ receptor ligands (SA4503 and haloperidol) having a moderate affinity (*K*i = 50.2 and 41.4 nM, respectively)[20] for VAChT at the dose of 500 nmol/kg significantly reduced the brain uptake of (–)-[^{11}C]OMV (60–70% of specific binding), but the same dose of sigma$_1$ receptor ligand, (+)-pentazocine, having a low affinity (*K*i = 315 nM)[20] for VAChT, did not. Haloperidol was sometimes used to evaluate whether the VAChT radioligands bind to sigma receptor.[10,12,31] The moderate affinity of haloperidol for VAChTs (*K*i = 41.4 nM)[20]; however, reasonably blocked the binding of the radioligands to VAChTs. Previously, we reported that [^{3}H](+)-pentazocine showed a lower brain uptake and lower specific binding by the modulation of P-glycoproteins.[32] Then, we performed a further blocking study by pretreatment with a large excess dose of (±)-pentazocine (50 μmol/kg), where the uptake of (–)-[^{11}C]OMV significantly decreased in all of the brain regions (44–75% of control). A low affinity of (+)-pentazocine (*K*i = 315 nM)[20] at the dose of 50 μmol/kg may also block the binding of (–)-[^{11}C]OMV to VAChTs. When comparing the blocking effects among the tissues

investigated, the uptake of (–)-[^{11}C]OMV in the striatum was decreased to a lesser extent by the co-injection of SA4503 (44% of control) and haloperidol (61% of control), as well as by the pretreatment with a large excess of (±)-pentazocine (75% of control). Although selective ligands for VAChT or sigma receptors were not applied to the blocking studies, (–)-[^{11}C]OMV mainly binds to VAChTs by considering the fact that the striatum has a high density of VAChTs and a low density of sigma$_1$ receptors,[30] and a part of the reduction by sigma receptor ligands reflects the binding of (–)-[^{11}C]OMV to sigma$_1$ receptors with a moderate affinity (*K*i = 34 nM).[20] On the other hand, in the cerebellum, a 70% reduction of uptake of (–)-[^{11}C]OMV by SA4503 and a lesser reduction by (–)-OMV and (–)-vesamicol reflect that (–)-[^{11}C]OMV mainly binds to the sigma$_1$ receptors because of the low density of VAChT. With regard the non-specific binding of (–)-[^{11}C]OMV, 30–35% of the total uptake maximally remained in the blocking study. These levels of the non-specific binding of (–)-[^{11}C]OMV were similar to those of [^{11}C]SA4503,[24] suggesting that the non-specific binding would not hamper the specific signals of the tracer in the human brain by PET.[25]

In an imaging study with *ex vivo* autoradiography in rats, the regional brain distribution of (–)-[^{11}C]OMV was similar to that of [^{3}H](–)-vesamicol,[33] but not to that of [^{11}C]SA4503.[23] In the PET measurement of the monkey brain, the uptake of (–)-[^{11}C]OMV was relatively higher in the striatum, being rich in VAChTs, and the regional distribution pattern of (–)-[^{11}C]OMV was similar to that of [^{18}F](+)-4-fluorobenzyltrozamicol as a PET ligand for VAChT sites,[34] but different from that of [^{11}C]SA4503 as a PET ligand for the sigma$_1$ receptor.[24] In the striatum, the density of VAChT was high,[29] and that of the sigma$_1$ receptor was low.[35] Therefore, the findings suggest that the binding of (–)-[^{11}C]OMV to VAChTs is a major contribution to the PET images in the striatum.

In conclusion, (–)-[^{11}C]OMV was prepared in sufficient yield and with specific activity for *in vivo* studies by methylation of (–)-*o*-trimethylstannyl-vesamicol with [^{11}C]methyl iodide in a palladium-promoted cross-coupling reaction. (–)-[^{11}C]OMV showed a high brain uptake and appropriate brain kinetics during the time frame of ^{11}C-labeled tracers, and bound mainly to VAChTs; however, the binding of the tracer to sigma$_1$ receptors due to a low affinity (*K*i for sigma$_1$, 33.7 nM)[20] was not disregarded. Therefore, (–)-[^{11}C]OMV-PET together with help of [^{11}C]SA4503-PET may evaluate VAChTs.

ACKNOWLEDGMENTS

The authors thank Dr. QingGeLeTu for his technical assistance in the autoradiography study, and also thank the staff of Positron Medical Center, Tokyo Metropolitan Institute of Gerontology and the staff of Central Research Laboratory, Hamamatsu Photonics K.K. This work was supported in part by Grant-in-Aid for Creative Scientific Research of the Japan Society for the Promotion of Science.

REFERENCES

1. Schafer MK, Weihe E, Varoqui H, Eiden LE, Erickson JD. Distribution of the vesicular acetylcholine transporter (VAChT) in the central and peripheral nervous systems of the rat. *J Mol Neurosci* 1994; 5: 1–26.
2. Schafer MK, Weihe E, Erickson JD, Eiden LE. Human and monkey cholinergic neurons visualized in paraffin-embedded tissues by immunoreactivity for VAChT, the vesicular acetylcholine transporter. *J Mol Neurosci* 1995; 6: 225–235.
3. Gilmor ML, Nash NR, Roghani A, Edwards RH, Yi H, Hersch SM, et al. Expression of the putative vesicular acetylcholine transporter in rat brain and localization in cholinergic synaptic vesicles. *J Neurosci* 1996; 16: 2179–2190.
4. Weihe E, Tao-Cheng JH, Schafer MK, Erickson JD, Eiden LE. Visualization of the vesicular acetylcholine transporter in cholinergic nerve terminals and its targeting to a specific population of small synaptic vesicles. *Proc Natl Acad Sci USA* 1996; 93: 3547–3552.
5. Bahr BA, Parsons SM. Acetylcholine transport and drug inhibition kinetics in Torpedo synaptic vesicles. *J Neurochem* 1986; 46: 1214–1218.
6. Marshall IG, Parsons SM. The vesicular acetylcholine transport system. *Trends Neurosci* 1987; 10: 174–177.
7. Kilbourn MR, Jung YW, Haka MS, Gildersleeve DL, Kuhl DE, Wieland DM. Mouse brain distribution of a carbon-11 labeled vesamicol derivative: presynaptic marker of cholinergic neurons. *Life Sci* 1990; 47: 1955–1963.
8. DeGrado TR, Mulholland GK, Wieland DM, Schwaiger M. Evaluation of (–)[^{18}F]fluoroethoxybenzovesamicol as a new PET tracer of cholinergic neurons of the heart. *Nucl Med Biol* 1994; 21: 189–195.
9. Rogers GA, Stone-Elander S, Ingvar M, Eriksson L, Parsons SM, Widen L. ^{18}F-labelled vesamicol derivatives: syntheses and preliminary *in vivo* small animal positron emission tomography evaluation. *Nucl Med Biol* 1994; 21: 219–230.
10. Efange SM, Mach RH, Khare A, Michelson RH, Nowak PA, Evora PH. *p*-[^{18}F]fluorobenzyltrozamicol ([^{18}F]FBT): molecular decomposition-reconstitution approach to vesamicol receptor radioligands for positron emission tomography. *Appl Radiat Isot* 1994; 45: 465–472.
11. Efange SM, Mach RH, Smith CR, Khare AB, Foulon C, Akella SK, et al. Vesamicol analogues as sigma ligands. Molecular determinants of selectivity at the vesamicol receptor. *Biochem Pharmacol* 1995; 49: 791–797.
12. Mulholland GK, Wieland DM, Kilbourn MR, Frey KA, Sherman PS, Carey JE, et al. [^{18}F]fluoroethoxy-benzovesamicol, a PET radiotracer for the vesicular acetylcholine transporter and cholinergic synapses. *Synapse* 1998; 30: 263–274.
13. Efange SM, Nader MA, Ehrenkaufer RL, Khare AB, Smith CR, Morton TE, et al. (+)-*p*-([^{18}F]fluorobenzyl)spirotrozamicol [(+)-[^{18}F]spiro-FBT]: synthesis and biological evaluation of a high-affinity ligand for the vesicular acetylcholine transporter (VAChT). *Nucl Med Biol* 1999; 26:

189–192.
14. Jung YW, Van Dort ME, Gildersleeve DL, Wieland DM. A radiotracer for mapping cholinergic neurons of the brain. *J Med Chem* 1990; 33: 2065–2068.
15. Efange SM, Michelson RH, Khare AB, Thomas JR. Synthesis and tissue distribution of (*m*-[^{125}I]iodobenzyl)trozamicol ([^{125}I]MIBT): potential radioligand for mapping central cholinergic innervation. *J Med Chem* 1993; 36: 1754–1760.
16. Shiba K, Mori H, Matsuda H, Tsuji S, Kuji I, Sumiya H, et al. Synthesis of radioiodinated analogs of 2-(4-phenylpiperidino)cyclohexanol (vesamicol) as vesamicol-like agent. *Nucl Med Biol* 1995; 22: 205–210.
17. Khare AB, Langason RB, Parsons SM, Mach RH, Efange SM. *N*-(3-Iodophenyl)trozamicol (IPHT) and related inhibitors of vesicular acetylcholine transport: synthesis and preliminary biological characterization. *Nucl Med Biol* 1999; 26: 609–617.
18. Bando K, Taguchi K, Ginoza Y, Naganuma T, Tanaka Y, Koike K, et al. Synthesis and evaluation of radiolabeled piperazine derivatives of vesamicol as SPECT agents for cholinergic neurons. *Nucl Med Biol* 2001; 28: 251–260.
19. Shiba K, Yano T, Sato W, Mori H, Tonami N. Characterization of radioiodinated (−)-ortho-iodovesamicol binding in rat brain preparations. *Life Sci* 2002; 71: 1591–1598.
20. Shiba K, Ogawa K, Ishiwata K, Yajima K, Mori H. Synthesis and binding affinities of methyl vesamicol analogs for the acetylcholine transporter and sigma receptor. *Bioorg Med Chem* 2006; 14: 2620–2626.
21. Mach RH, Voytko ML, Ehrenkaufer RL, Nader MA, Tobin JR, Efange SM, et al. Imaging of cholinergic terminals using the radiotracer [^{18}F](+)-4-fluorobenzyltrozamicol: *in vitro* binding studies and positron emission tomography studies in nonhuman primates. *Synapse* 1997; 25: 368–380.
22. Suzuki M, Doi H, Björkman M, Andersson Y, Långström B, Watanabe Y, et al. Rapid coupling of methyl iodide with aryltributylstannanes mediated by palladium(0) complexes: a general protocol for the synthesis of $^{11}CH_3$-labeled PET tracers. *Chem Eur J* 1997; 3: 2039–2042.
23. Kawamura K, Ishiwata K, Tajima H, Ishii S, Matsuno K, Homma Y, et al. *In vivo* evaluation of [^{11}C]SA4503 as a PET ligand for mapping CNS sigma$_1$ receptors. *Nucl Med Biol* 2000; 27: 255–261.
24. Kawamura K, Kimura Y, Tsukada H, Kobayashi T, Nishiyama S, Kakiuchi T, et al. An increase of sigma$_1$ receptors in the aged monkey brain. *Neurobiol Aging* 2003; 24; 745–752.
25. Mishina M, Ishiwata K, Ishii K, Kitamura S, Kimura Y, Kawamura K, et al. Function of sigma$_1$ receptors in Parkinson's disease. *Acta Neulologica* 2005; 112: 103–107.
26. Samuelsson L, Långström B. Synthesis of 1-(2′-deoxy-2′-fluoro-β-D-arabinofuranosyl)-[methyl-^{11}C]thimine ([^{11}C]FMAU) via a still cross-coupling reaction with [^{11}C]methyl iodide. *J Label Compd Radiopharm* 2003; 46: 263–272.
27. Custers FG, Leysen JE, Stoof JC, Herscheid JD. Vesamicol and some of its derivatives: questionable ligands for selectively labelling acetylcholine transporters in rat brain. *Eur J Pharmacol* 1997; 338: 177–183.
28. Frey KA, Wieland DM, Kilbourn MR. Imaging of monoaminergic and cholinergic vesicular transporters in the brain. *Adv Pharmacol* 1998; 42: 269–272.
29. Efange SM. *In vivo* imaging of the vesicular acetylcholine transporter and the vesicular monoamine transporter. *FASEB J* 2000; 14: 2401–2413.
30. Bouchard P, Quirion R. [^{3}H]1,3-di(2-tolyl)guanidine and [^{3}H](+)pentazocine binding sites in the rat brain: autoradiographic visualization of the putative sigma$_1$ and sigma$_2$ receptor subtypes. *Neuroscience* 1997; 76: 467–477.
31. Efange SM, von Hohenberg K, Khare AB, Tu Z, Mach RH, Parsons SM. Synthesis and biological characterization of stable and radioiodinated (+/−)-trans-2-hydroxy-3-P[4-(3-iodophenyl)piperidyl]-1,2,3,4-tetrahydronaphthalene (3′-IBVM). *Nucl Med Biol* 2000; 27: 749–755.
32. Kawamura K, Kobayashi T, Matsuno K, Ishiwata K. Different brain kinetics of two sigma$_1$ receptor ligands, [^{3}H](+)-pentazocine and [^{11}C]SA4503, by P-glycoprotein modulation. *Synapse* 2003; 48: 80–86.
33. Shiba K, Mori H, Matsuda H, Tsuji S, Tonami N, Hisada K. *In vivo* characterization of radioiodinated 2-(4-phenylpiperidino)cyclohexanol (vesamicol) analogs: potential radioligand for mapping presynaptic cholinergic neurons. *Nucl Med Biol* 1995; 22: 823–828.
34. Gage HD, Voytko ML, Ehrenkaufer RL, Tobin JR, Efange SM, Mach RH. Reproducibility of repeated measures of cholinergic terminal density using [^{18}F](+)-4-fluorobenzyltrozamicol and PET in the rhesus monkey brain. *J Nucl Med* 2000; 41: 2069–2076.
35. Mash DC, Zabetian CP. Sigma receptors are associated with cortical limbic areas in the primate brain. *Synapse* 1992; 12: 195–205.